

# RSC Advances



This is an *Accepted Manuscript*, which has been through the Royal Society of Chemistry peer review process and has been accepted for publication.

*Accepted Manuscripts* are published online shortly after acceptance, before technical editing, formatting and proof reading. Using this free service, authors can make their results available to the community, in citable form, before we publish the edited article. This *Accepted Manuscript* will be replaced by the edited, formatted and paginated article as soon as this is available.

You can find more information about *Accepted Manuscripts* in the [Information for Authors](#).

Please note that technical editing may introduce minor changes to the text and/or graphics, which may alter content. The journal's standard [Terms & Conditions](#) and the [Ethical guidelines](#) still apply. In no event shall the Royal Society of Chemistry be held responsible for any errors or omissions in this *Accepted Manuscript* or any consequences arising from the use of any information it contains.

1     **Hydrogen evolution inhibition by L-Serine at the negative electrode**  
2                                   **of a lead-acid battery**

3                                   **M. A. Deyab\***

4     \*Egyptian Petroleum Research Institute (EPRI), Nasr City, Cairo, Egypt

5     \* Corresponding author. Tel.: +201006137150; fax: + 202 22747433

6                                   E-mail address: hamadadeiab@yahoo.com

7     **Abstract**

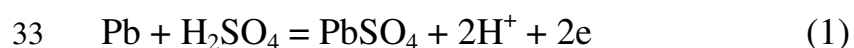
8     The inhibition effect of L-Serine on the hydrogen evolution at the  
9     negative electrode of a lead-acid battery (Pb) in 5.0 M H<sub>2</sub>SO<sub>4</sub> has been  
10    studied by hydrogen evolution and electrochemical methods. The surface  
11    of Pb is analyzed with scanning electron microscope (SEM) and energy-  
12    dispersive X-ray (EDX). The results demonstrate that L-Serine is an  
13    adequate inhibitor, retarding the hydrogen evolution reaction.  
14    Polarization curves denote that L-Serine performs as the cathodic  
15    inhibitor. The inhibition efficiency boosts with increase in L-Serine  
16    concentration but decreases with upturn in temperature. The most  
17    efficient inhibitor concentration is 10 mM. Adsorption of L-Serine on the  
18    Pb surface is unprompted and complies with Langmuir's isotherm. L-  
19    Serine induces an energy barrier for the hydrogen evolution reaction and  
20    this barrier increases with increasing L-Serine concentration.

21    **Keywords:** hydrogen evolution; lead-acid battery; inhibition; amino acid

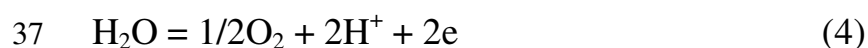
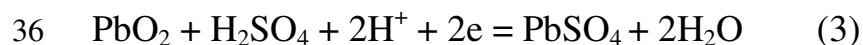
## 22 1. Introduction

23 The lead–acid battery is the oldest type of rechargeable battery [1-2]. It  
24 consists of PbO<sub>2</sub> as a positive electrode, Pb as a negative electrode and an  
25 electrolyte of aqueous H<sub>2</sub>SO<sub>4</sub>. The concentration of H<sub>2</sub>SO<sub>4</sub> in a fully  
26 charged auto battery measures a specific gravity of 1.265 – 1.285 [2].  
27 This is equivalent to a molar concentration of 4.5 – 6.0 M. As the battery  
28 discharges, PbO<sub>2</sub> and Pb react with aqueous solution of H<sub>2</sub>SO<sub>4</sub> to form  
29 PbSO<sub>4</sub> and water. On recharge, PbSO<sub>4</sub> converts back to PbO<sub>2</sub> and Pb. In  
30 the same time, SO<sub>4</sub><sup>2-</sup> ions are driven back into the electrolyte solution to  
31 form H<sub>2</sub>SO<sub>4</sub>. The reactions can be presented as the following:

32 At the negative electrode [3]:



35 At the positive electrode:



38 Under normal conditions, gassing vented from a lead-acid battery is  
39 mainly oxygen and hydrogen gas [4-5].

40 Hydrogen gas can collect at the top of a battery. If this gas is exposed  
41 to a flame or spark, it can explode. Hydrogen gas evolution harm the  
42 valve regulated lead acid battery during charging and discharging

43 processes [6]. In addition to the primary focus on human and system  
44 safety, hydrogen evolution also affects on the battery life and  
45 maintenance economics. Therefore the inhibition of hydrogen evolution  
46 during the charging of a lead-acid battery is an important part of the  
47 engineering for any battery system [7-10].

48 The aim of this work is to explore the use of L-Serine to inhibit the  
49 hydrogen evolution during the reaction of Pb with 5.0 M H<sub>2</sub>SO<sub>4</sub>.

50 L-serine is a non essential amino acid. It is manufactured by  
51 fermentation from carbohydrate sources [11]. In contrast to most  
52 commercial acid corrosion inhibitors which are highly toxic, L-serine is  
53 an environmentally friendly corrosion inhibitor. However, there is no  
54 literature to date about the corrosion inhibitory effect of L-serine in acid  
55 solution.

## 56 **2. Experimental**

### 57 **2.1. Materials**

58 The working electrodes were made from pure lead (Pb) 99.99%.  
59 Specimens used for hydrogen evolution measurements were mechanically  
60 cut into 2.0 × 1.0 × 0.2 cm dimensions. For electrochemical  
61 measurements, the cylindrical rod of Pb with exposed surface area of  
62 0.452 cm<sup>2</sup> was allowed to contact the test solutions. The working  
63 electrodes were abraded with different grads of emery papers up to 1200

64 grad. Then they were cleaned by using acetone and distilled water before  
65 the tests.

66 Experiments were done in 5.0 M H<sub>2</sub>SO<sub>4</sub> in the absence and presence  
67 of L-Serine. L-Serine was obtained commercially from Sigma-Aldrich  
68 Co.

69 All solutions were prepared from analytical grade chemicals and  
70 distilled water. The temperature of the solutions was controlled by a  
71 thermostat.

## 72 **2.2. Hydrogen evolution rate measurements**

73 The schematic diagram of the hydrogen evolution measurements was  
74 reported in previous paper [12]. The volume of H<sub>2</sub> gas evolved ( $\Delta V$ )  
75 during the reaction of Pb specimens in 100 ml of 5.0 M H<sub>2</sub>SO<sub>4</sub> was  
76 measured at specified time intervals ( $t$ ). The hydrogen evolution rate ( $H_R$ )  
77 was expressed using the following correlation [13]:

$$78 \quad H_R = (\Delta V) / (t) \quad (5)$$

## 79 **2.3. Electrochemical measurements**

80 Electrochemical experiments (Potentiodynamic polarization) were  
81 performed in a regular three-electrode cell. A platinum coil was used as  
82 the counter electrode and potentials were measured relative to Hg/Hg<sub>2</sub>SO<sub>4</sub>  
83 reference electrode. Electrochemical experiments were conducted using  
84 Potentiostat/Galvanostat (Gill AC model no. 947, ACM instruments).

85 Before electrochemical measurements, the Pb electrode was immersed in  
86 freshly prepared solutions at open circuit potential (OCP) for 2 h, to attain  
87 a steady case. The potential of polarization curves was done from - 200  
88 mV to + 200 mV versus OCP with  $1.0 \text{ mV s}^{-1}$  sweep rate.

#### 89 **2.4. SEM-EDX analysis**

90 The surface morphology of the metal specimen was evaluated by SEM-  
91 EDX analysis using JOEL-JEM-1200 EX II ELETRON MICROSCOPE  
92 and a Traktor TN-2000 energy dispersive spectrometer.

### 93 **3. Results and discussion**

#### 94 **3.1. Effect of L-Serine concentration on the hydrogen evolution**

95 The effect of the addition of various concentrations of L-Serine (0.1-20  
96 mM) on the  $H_R$  during the reaction of Pb in 5.0 M  $\text{H}_2\text{SO}_4$  at 303 K is  
97 shown in Fig. 1. It should be noted that the presence of L-Serine in 5.0 M  
98  $\text{H}_2\text{SO}_4$  has a considerable influence on the inhibition of the hydrogen  
99 evolution rates  $H_R$ . Furthermore, increasing the concentration of L-Serine  
100 from 0.1 to 20 mM causes a noticeable decrease in hydrogen evolution  
101 rates  $H_R$ .

102 The efficiency of L-Serine ( $I_H \%$ ) to inhibit the hydrogen evolution is  
103 calculated according to [13] :

$$104 \quad I_H \% = \left( 1 - \frac{H_R}{H_{R_0}} \right) \times 100 \quad (6)$$

105 where  $H_{R0}$  and  $H_R$  are the hydrogen evolution rates without and with L-  
106 Serine, respectively.

107 Fig. 2 shows variations of the efficiency of L-Serine  $I_H \%$  as a function  
108 of the logarithmic of L-Serine concentration. The plot of Fig. 2 exhibits  
109 S-shaped adsorption isotherm. This suggests, but does not prove, that L-  
110 Serine inhibits the hydrogen evolution during the reaction of Pb in 5.0 M  
111  $H_2SO_4$  by adsorption at the Pb/  $H_2SO_4$  solution interface [14]. It is evident  
112 from Fig. 2 that upon increasing L-Serine concentration to 10 mM,  $I_H \%$   
113 values significantly increases reaching a maximum value ( $I_H \% = 88$ ).  
114 However, a further increase in L-Serine concentration to 20 mM does not  
115 lead to a change in  $I_H \%$  values. This may be due to the adsorption of L-  
116 Serine on the surface of Pb have reached the state of equilibrium at 10  
117 mM and consequently, any further addition will not yield any increase in  
118 the inhibition efficiency [15]

### 119 **3.2. Effect of temperature and activation energy calculation**

120 The rate of the chemical reactions inside the lead-acid battery depends  
121 on the temperature. In general, the increase of the temperature causes the  
122 acceleration in the reaction rate of the internal processes, e.g. corrosion  
123 (aging), self discharge and the corresponding hydrogen and oxygen gas  
124 evolution rates [16-17].

125 To assess the influence of temperature on the hydrogen evolution rate  
126 and the hydrogen evolution inhibition process, the hydrogen evolution  
127 rates  $H_R$  are performed at different temperatures (303 and 323 K) without  
128 and with different concentrations of L-Serine. The results are recorded in  
129 Table 1. The results obtained indicate that the rates of the hydrogen  
130 evolution rate in all cases increased with temperature while  $I_H$  %  
131 decreased. The increase in the  $H_R$  in the absence of L-Serine with the rise  
132 of temperature may be arises from an increase in  $PbSO_4$  solubility with  
133 temperature [18]. In the same time, the raise in temperature accelerates  
134 both of the diffusion and migration rates for the reactant and product  
135 species. This drives to an increase in the rate of hydrogen evolution  
136 reaction. On the other hand, the increase in the  $H_R$  and the decrease in the  
137  $I_H$  % in the presence of L-Serine with the rise of temperature may be  
138 assign to the partial desorption of L-Serine molecules from Pb surface  
139 with temperature [19].

140 The activation energy ( $E_a$ ) for the process responsible for hydrogen  
141 generation (diffusion of both protons and uncharged hydrogen in  
142 solution) was computed using the Arrhenius relation [13]:

$$143 \quad E_a = 2.303R \frac{\log\left(\frac{H_{R2}}{H_{R1}}\right)}{\left(\frac{1}{T_1} - \frac{1}{T_2}\right)} \quad (7)$$

144 where  $R$  is the ideal gas constant,  $H_{R1}$  and  $H_{R2}$  are the hydrogen evolution  
145 rates at the absolute temperatures  $T_1$  and  $T_2$ , respectively.

146 The calculated values of  $E_a$  are recorded in Table 1.

147 The data examination shows that the activation energy is higher in the  
148 presence of L-Serine than in its absence. The higher  $E_a$  value in the  
149 presence of L-Serine, implies that physical adsorption exists between L-  
150 Serine molecules and the charged surface. Moreover, the values of  $E_a$   
151 increase with increasing L-Serine concentration. This means that, the  
152 presence of L-Serine induces an energy barrier for the hydrogen evolution  
153 reaction and this barrier increases with increasing concentration of L-  
154 Serine [20].

### 155 **3.3. Electrochemical measurements**

156 Fig. 3 shows anodic and cathodic polarization plots (Tafel plots)  
157 recorded on Pb electrode in 5.0 M  $H_2SO_4$  containing different  
158 concentrations of L-Serine at 303 K.

159 It can be noticed that the addition of L-Serine causes a remarkable  
160 decrease in the corrosion rate.

161 It is clear that, the presence of L-Serine shifts cathodic curves to lower  
162 values of current densities. Whereas the anodic curves are slightly  
163 retarded by L-Serine. This result suggests that the addition of L-Serine  
164 retards the hydrogen evolution reaction [21].

165 Table 2 displays the kinetic parameters for corrosion process, i.e.,  
166 corrosion potential ( $E_{\text{corr}}$ ) and corrosion current density ( $j_{\text{corr}}$ ) [22].

167 Comparing with blank solution,  $E_{\text{corr}}$  shifts to negative side more than  
168 85 mV in the presence of L-Serine; this elucidates that L-Serine works as  
169 cathodic-type inhibitor [23]. Evidently,  $j_{\text{corr}}$  decreases frequently in the  
170 presence of L-Serine and decreases with L-Serine concentration. The  
171 corrosion current density  $j_{\text{corr}}$  values can be used to calculate the inhibition  
172 performances of L-Serine ( $\eta_j$  %) from the following equation [24] :

$$173 \quad \eta_j \% = \frac{j_{\text{corr}(0)} - j_{\text{corr}}}{j_{\text{corr}(0)}} \times 100 \quad (8)$$

174 where  $j_{\text{corr}(0)}$  and  $j_{\text{corr}}$  are uninhibited and inhibited current densities,  
175 respectively.

176 From results given in Table 2, an increase of  $\eta_j$  % with L-Serine  
177 concentration, reaching a maximum value (91%) at 10 mM, was  
178 observed. A slight a change in  $\eta_j$  % values was found above the 10 mM.  
179 This phenomenon is consistent with results obtained form hydrogen  
180 evolution measurements.

### 181 **3.4. Study of the adsorption phenomenon**

182 The adsorption isotherms can supply helpful information about the  
183 mechanism of corrosion inhibition [25-26].

184 The degree of surface coverage ( $\theta$ ) of L-Serine from hydrogen  
185 evolution and electrochemical measurements can be calculated using the  
186 following equations [27]:

$$187 \quad \theta = \left( 1 - \frac{H_R}{H_{Ro}} \right) \quad (9)$$

$$188 \quad \theta = \frac{j_{\text{corr}(0)} - j_{\text{corr}}}{j_{\text{corr}(0)}} \quad (10)$$

189 The surface coverage values  $\theta$  were fitted to different adsorption  
190 isotherm models and best results judged by the correlation coefficient  
191 ( $R^2$ ) were obtained with Langmuir adsorption isotherm as follows [28]:

$$192 \quad \frac{C_{\text{inh}}}{\theta} = \frac{1}{K_{\text{ads}}} + C_{\text{inh}} \quad (11)$$

193 where  $C_{\text{inh}}$  is L-Serine concentration and  $K_{\text{ads}}$  is Langmuir isotherm  
194 constant.

195 The plot of  $C_{\text{inh}} / \theta$  versus  $C_{\text{inh}}$  (Fig. 4) yields a straight lines with a  
196 correlation coefficients ( $R^2$ ) are close to one (Table 3). This supports the  
197 assumption that the adsorption of L-Serine from 5.0 M  $\text{H}_2\text{SO}_4$  solution on  
198 the Pb surface at the studied temperatures comply with the Langmuir  
199 adsorption isotherm [29]. The high values of  $K_{\text{ads}}$  (Table 3) reflect the  
200 high adsorption efficiency of L-Serine on Pb surface [30].  $K_{\text{ads}}$  can be  
201 used to determine the free Gibbs energy of adsorption ( $\Delta G_{\text{ads}}^0$ ) using the  
202 following equation [31]:

$$\Delta G_{\text{ads}}^0 = -RT \ln (55.5 K_{\text{ads}}) \quad (12)$$

The calculated  $\Delta G_{\text{ads}}^0$  values obtained from hydrogen evolution and electrochemical data were given in Table 3. The data clearly show that  $\Delta G_{\text{ads}}^0$  values were negative. In essence, this means that the adsorption of L-Serine molecules on Pb surface will be favored and will release energy. Furthermore, the values  $\Delta G_{\text{ads}}^0$  of less than  $-40 \text{ kJ mol}^{-1}$  indicate physical adsorption [32].

The heat of adsorption ( $Q_{\text{ads}}$ ) of L-Serine on Pb surface has been determined as a function of the surface coverage ( $\theta$ ) and temperature as follows [33]:

$$Q_{\text{ads}} = 2.303R \left( \log \frac{\theta_2}{1-\theta_2} - \log \frac{\theta_1}{1-\theta_1} \right) \times \left( \frac{T_1 T_2}{T_2 - T_1} \right) \quad (13)$$

where  $\theta_1$  and  $\theta_2$  are the degrees of surface coverage ( $\theta_1$  and  $\theta_2$  values were calculated using equation 9) at  $T_1$  and  $T_2$ , respectively.

The calculated values for  $Q_{\text{ads}}$  are presented in Table 4. The negative value of  $Q_{\text{ads}}$  assumes that the adsorption process is exothermic and physisorption [33].

### 3.5. SEM-EDX examinations

The aim of SEM-EDX examinations was to confirm the results obtained from the hydrogen evolution and electrochemical measurements that a protective surface film of L-Serine molecules is formed on the Pb

223 surface. To attain this aim, SEM-EDX examinations of the Pb surface  
224 were performed in 5.0 M H<sub>2</sub>SO<sub>4</sub> in the absence and presence of 20 mM of  
225 L-Serine.

226 As it is shown in Fig. 5a, the Pb surface was strongly damaged in the  
227 absence of L-Serine due to Pb corrosion in 5.0 M H<sub>2</sub>SO<sub>4</sub>. However, less  
228 corrosion attack was found for the sample exposed to H<sub>2</sub>SO<sub>4</sub> solution  
229 containing L-Serine (Fig.5b). A smoother surface is seen in the presence  
230 of 20 mM L-Serine in comparison to that observed in Fig.5a.

231 Fig. 6 presents EDX survey spectra recorded for Pb surface exposed  
232 for 5.0 M H<sub>2</sub>SO<sub>4</sub> in the absence and presence of 20 mM L-Serine. In  
233 H<sub>2</sub>SO<sub>4</sub> solution free solution, the EDX spectra (Fig. 6a) show the  
234 characteristics peaks of Pb element. In addition, PbSO<sub>4</sub> is present, as  
235 indicated by the Pb, S and O signals. In solution contain 20 mM L-Serine  
236 (Fig. 6b), the EDX spectra showed an additional line characteristic for the  
237 existence of N and C. In addition, the intensity of S signal decreased. The  
238 appearance of the N and C signals is due to the N and C atoms of the  
239 adsorbed L-Serine molecules.

240 These data confirm the adsorption of L-Serine molecules on the Pb  
241 surface and formulation a protective surface film.

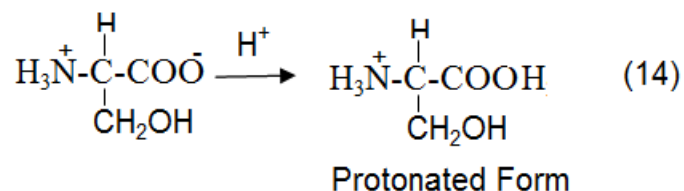
### 242 **3.6. Explanation for inhibition**

243 The effectiveness of organic inhibitor may be due to the adsorption of  
244 inhibitor molecules on the metal surface [34-35]. Adsorption process  
245 occurs through the electrostatic attractive forces between dipoles and/or  
246 ionic charges on the adsorbed molecules and the electric charge on the  
247 metal surface. The presence of heteroatoms with loosely bound electrons  
248 or  $\pi$ -electron systems or aromatic rings in molecular structure of the  
249 inhibitor enhance the adsorption efficiency process [36-37].

250 In acidic solutions the anodic reaction produces metal ions, and the  
251 principal cathodic reaction produces hydrogen gas. An inhibitor may  
252 decrease the metal dissolution, hydrogen gas evolution, or both processes.  
253 The shift of the corrosion potential to the positive direction indicates  
254 mainly inhibition of the metal dissolution process (anodic inhibitor),  
255 whereas the shift to the negative direction indicates mainly inhibition of  
256 the hydrogen gas evolution (cathodic inhibitor) [38].

257 In the present work, the essential step in the inhibition of hydrogen  
258 evolution during the reaction of Pb in 5.0 M  $\text{H}_2\text{SO}_4$  is the adsorption of L-  
259 Serine on cathodic sites on the Pb surface. L-Serine has three polar  
260 groups, namely,  $\text{NH}_2$ ,  $\text{COOH}$ , and  $\text{OH}$  groups. It can coordinate with Pb  
261 surface through the nitrogen atom and oxygen atom of the polar groups  
262 [39]. In neutral solutions, L-Serine molecules are presented usually as

263 Zwitter ions. Whereas in acidic solutions, L-Serine molecules are  
264 presented in protonated form as the following:



265

266 This means that in acidic medium, L-Serine molecules are adsorbed  
267 through the  $^+\text{NH}_3$  on the electrode surface (cathodic sites) and decrease  
268 the rate of the cathodic reaction, thus the rate of hydrogen evolution will  
269 be decreased.

#### 270 4. Conclusion

271 The inhibition performance of L-Serine on the hydrogen evolution at the  
272 negative electrode of a lead-acid battery (Pb) in 5.0 M  $\text{H}_2\text{SO}_4$  solution  
273 was evaluated using hydrogen evolution and electrochemical methods.  
274 The results show that L-Serine works as an adequate inhibitor for the  
275 hydrogen evolution at Pb electrode in 5.0 M  $\text{H}_2\text{SO}_4$ . The inhibition  
276 efficiency of L-Serine depends on its concentration and solution  
277 temperature. The results of electrochemical measurements demonstrate  
278 that L-Serine behaves as a cathodic-type inhibitor. The adsorption of L-  
279 Serine on Pb surface complies with Langmuir's isotherm. SEM and EDX  
280 analysis clearly show that the inhibitor molecules form a good protective  
281 film on the Pb surface.

282 **References**

- 283 [1] Bode H. Lead-Acid Batteries. John Wiley and Sons: New York,  
284 London; 1977.
- 285 [2] Linden D, Reddy TB. Handbook of Batteries (3rd Ed.). McGraw-Hill:  
286 New York; 2002.
- 287 [3] Kuhn AT. The Electrochemistry of Lead. John Wiley and Sons: New  
288 York; 1979.
- 289 [4] Berndt D. Valve-regulated lead-acid batteries. J Power Sources 2001;  
290 95: 2-12.
- 291 [5] Lam LT, Lim OV, Haigh NP, Rand DAJ, Manders JE, Rice DM.  
292 Oxide for valve-regulated lead-acid batteries. J Power Sources 1998;  
293 73: 36-46.
- 294 [6] Dietz H, Radwan M, Doring H, Wiesener K. On the hydrogen balance  
295 in sealed lead/acid batteries and its effect on battery performance. J  
296 Power Sources 1993; 42: 89-101.
- 297 [7] Mahato BK, Tiedemann WH. Linear Potential Sweep of Lead - Acid  
298 Battery Electrodes Containing Trace Te, Sb, As, Co, and Ni. J  
299 Electrochem Soc 1983; 130: 2139-2144.
- 300 [8] Maja N, Penazi N. Effect of some elements on oxygen reduction and  
301 hydrogen evolution at lead-acid battery negative plates. J Power  
302 Sources 1988; 22:1-9.

- 303 [9] Saakes M, Van Duin PJ, Ligtoet ACP, Schmal D. Investigations of  
304 the negative plate of lead/acid cells 1. Selection of additives. *J Power*  
305 *Sources* 1994; 47:129-147.
- 306 [10] Vijayamohanan K, Sathyanarayana S, Joshi SN. Kinetics of  
307 hydrogen evolution reaction on lead/acid battery negative electrodes  
308 with silicate and antimony added to the electrolyte. *J Power Sources*  
309 1990; 30:169-175.
- 310 [11] Dawson RMC. *Data for Biochemical Research*, Oxford: Clarendon  
311 Press; 1959.
- 312 [12] Deyab MA. Effect of halides ions on H<sub>2</sub> production during aluminum  
313 corrosion in formic acid and using some inorganic inhibitors to control  
314 hydrogen Evolution. *J Power Sources* 2013; 242:86-90.
- 315 [13] Deyab MA. Hydrogen generation during the corrosion of carbon  
316 steel in crotonic acid and using some organic surfactants to control  
317 hydrogen evolution. *Int J Hydrogen Energy* 2013; 38:13511-13519.
- 318 [14] Arab ST, Noor EA. Inhibition of Acid Corrosion of Steel by Some  
319 S-Alkylisothiuronium Iodides. *Corrosion* 1993; 49:122-129.
- 320 [15] Luo Z, Zhang S, Guo L. Investigation of a Pharmaceutically Active  
321 Compound Omeprazole as Inhibitor for Corrosion of Mild Steel in  
322 H<sub>2</sub>SO<sub>4</sub> Solution. *Int J Electrochem Sci* 2014; 9: 7309 – 7324.

- 323 [16] Siniard K, Xiao M, Choe S-Y One-dimensional dynamic modeling  
324 and validation of maintenance-free lead-acid batteries emphasizing  
325 temperature effects. *J Power Sources* 2010; 195: 7102-7114.
- 326 [17] Omae T, Osumi S, Takahashi K, Tsubota M. Negative corrosion of  
327 lead-antimony alloys in lead-acid batteries at high temperatures  
328 Negative corrosion of lead-antimony alloys in lead-acid batteries at  
329 high temperatures. *J Power Sources* 1997; 65: 65-70.
- 330 [18] Deyab MA. Hydrogen generation by tin corrosion in lactic acid  
331 solution promoted by sodium perchlorate. *J Power Sources* 2014; 268:  
332 765-770.
- 333 [19] Deyab MA, Abd El-Rehim SS. Influence of Polyethylene Glycols  
334 on the Corrosion Inhibition of Carbon Steel in Butyric Acid Solution:  
335 Weight Loss, EIS and Theoretical Studies. *Int J Electrochem Sci*  
336 2013; 8:12613 – 12627.
- 337 [20] Deyab MA. Effect of cationic surfactant and inorganic anions on  
338 the electrochemical behavior of carbon steel in formation water.  
339 *Corros Sci* 2007; 49: 2315–2328.
- 340 [21] Vračar LjM, Dražić DM. Adsorption and corrosion inhibitive  
341 properties of some organic molecules on iron electrode in sulfuric  
342 acid. *Corros Sci* 2002; 44:1669-1680.

- 343 [22] Deyab MA. Corrosion protection of aluminum bipolar plates with  
344 polyaniline coating containing carbon nanotubes in acidic medium  
345 inside the polymer electrolyte membrane fuel cellJ Power Sources  
346 2014; 268: 50-55.
- 347 [23] Yadav M, Kumar S, Bahadur I, Ramjugernath D. Electrochemical  
348 and Quantum Chemical Studies on Synthesized Phenylazopyrimidone  
349 Dyes as Corrosion Inhibitors for Mild Steel in a 15% HCl Solution. Int  
350 J Electrochem Sci 2014; 9: 3928 – 3950.
- 351 [24] Deyab MA, Abd El-Rehim SS. Effect of succinic acid on carbon  
352 steel corrosion in produced water of crude oil. J Taiwan Inst Chem E  
353 2014; 45: 1065–1072.
- 354 [25] Adamson AW. A Textbook of Physical Chemistry, 2nd Ed.  
355 Academic Press: New York; 1979.
- 356 [26] Deyab MA, Keera ST, El Sabagh SM. Chlorhexidine digluconate  
357 as corrosion inhibitor for carbon steel dissolution in emulsified diesel  
358 fuel. Corros Sci 2011; 53: 2592–2597.
- 359 [27] Keera ST, Deyab MA. Effect of some organic surfactants on the  
360 electrochemical behaviour of carbon steel in formation water. Colloids  
361 and Surfaces A Physicochem Eng Aspects 2005; 266:129–140.
- 362 [28] Langmuir I. The constitution and fundamental properties of solids  
363 and liquids. J Am Chem Soc 1916; 38: 2221–2295.

- 364 [29] Kosari A, Moayed MH, Davoodi A, Parvizi R, Momeni M, Eshghi  
365 H, Moradi H. Electrochemical and quantum chemical assessment of  
366 two organic compounds from pyridine derivatives as corrosion  
367 inhibitors for mild steel in HCl solution under stagnant condition and  
368 hydrodynamic flow. *Corros Sci* 2014; 78:138–150.
- 369 [30] Döner A, Solmaz R, Özcan M, Kardaş G. Experimental and  
370 theoretical studies of thiazoles as corrosion inhibitors for mild steel in  
371 sulphuric acid solution. *Corros Sci* 2011; 53: 2902–2913.
- 372 [31] Foad El-Sherbini EE, Abd-El-Wahab SM, Deyab MA. Studies on  
373 corrosion inhibition of aluminum in 1.0 M HCl and 1.0 M H<sub>2</sub>SO<sub>4</sub>  
374 solutions by ethoxylated fatty acids. *Mater Chem Phys* 2003; 82: 631–  
375 637.
- 376 [32] Aljourani J, Raeissi K, Golozar MA. Benzimidazole and its  
377 derivatives as corrosion inhibitors for mild steel in 1M HCl solution.  
378 *Corros Sci* 2009; 51: 1836–1843.
- 379 [33] Deyab MA. Adsorption and inhibition effect of Ascorbyl palmitate  
380 on corrosion of carbon steel in ethanol blended gasoline containing  
381 water as a contaminant. *Corros Sci* 2014; 80: 359–365.
- 382 [34] Deyab MA, Abd El-Rehim SS, Keera ST. Study of the effect of  
383 association between anionic surfactant and neutral copolymer on the  
384 corrosion behaviour of carbon steel in cyclohexane propionic acid.

385 Colloids and Surfaces A Physicochem Eng Aspects 2009; 348: 170–  
386 176.

387 [35] Solmaz R. Investigation of corrosion inhibition mechanism and  
388 stability of Vitamin B1 on mild steel in 0.5 M HCl solution. Corros  
389 Sci 2014; 81: 75–84.

390 [36] Fragoza-Mar LF, Olivares-Xomet O, Dominguez-Aguilar MA,  
391 Flores EA, Arellanes-Lozada P, Jimenez-Cruz F. Corrosion inhibitor  
392 activity of 1,3-diketone malonates for mild steel in aqueous  
393 hydrochloric acid solution. Corros Sci 2012; 61: 171–184.

394 [37] Bockris JO'M, Reddy AKN. Modern Electrochemistry, vol. 2,  
395 Plenum Publishing Corporation:New York; 1976.

396 [38] Su W, Tang B, Fu F, Huang S, Zhao S, Bin L, Ding J, Chen C. A  
397 new insight into resource recovery of excess sewage sludge:  
398 Feasibility of extracting mixed amino acids as an environment-  
399 friendly corrosion inhibitor for industrial pickling. J Hazard Mater  
400 2014; 279:38-45.

401 [39] Meisenberg G, Simmons WH. Principles of Medical Biochemistry.  
402 3rd ed. Saunders-Elsevier; 2011.

403

404

405

406 **List of Figures**

407 Fig. 1 Variation of hydrogen evolution rate  $H_R$  with L-Serine  
408 concentration for Pb in 5.0 M  $H_2SO_4$  at 303 K.

409 Fig. 2 Variation of the efficiency of L-Serine  $I_H$  % as a function of the  
410 logarithmic concentration of L-Serine.

411 Fig. 3 Tafel polarization curves for Pb electrode in 5.0 M  $H_2SO_4$   
412 containing different concentrations of L-Serine at 303 K.

413 Fig. 4 Langmuir adsorption isotherm plot for adsorption of L-Serine on  
414 the Pb surface at 303 K.

415 Fig. 5 SEM images of Pb exposed to 5.0 M  $H_2SO_4$  in the absence (a)  
416 and presence of 20 mM of L-Serine (b).

417 Fig. 6 The EDX spectra of Pb in 5.0 M  $H_2SO_4$  in the absence (a) and  
418 presence of 20 mM of L-Serine (b).

**Table 1:** The values of hydrogen evolution rates ( $H_R$ ) at 303 and 323K, and activation energy ( $E_a$ ) for Pb in 5.0 M  $H_2SO_4$  in the absence and presence of various concentrations of L-Serine.

L-Serine (mM)	$H_{R1}$ (ml/h)	$H_{R2}$ (ml/h)	$E_a$ (kJ mol <sup>-1</sup> )
	303 K	323 K	
Blank	25	38	16.92
0.1	23	36	18.09
0.5	17	27	18.68
1	7	14	27.99
5	4	9	32.75
10	3	8	39.61
15	3	7	34.22
20	3	7	34.22

**Table 2** Polarization parameters for Pb in 5.0 M H<sub>2</sub>SO<sub>4</sub> without and with various concentrations of L-Serine.

L-Serine (mM)	$E_{\text{corr}}$ (mV vs. Hg/Hg <sub>2</sub> SO <sub>4</sub> )	$j_{\text{corr}}$ (mA cm <sup>-2</sup> )	$\eta_i$ %
Blank	-940	5.12	-
0.1	-1030	4.60	10.15
0.5	-1045	3.35	34.57
1	-1071	1.25	75.58
5	-1087	0.696	86.40
10	-1112	0.460	91.01
15	-1123	0.452	91.17
20	-1130	0.450	91.21

**Table 3** Adsorption parameters for L-Serine adsorption on Pb surface in 5.0 H<sub>2</sub>SO<sub>4</sub> at 303 K.

<b>Method</b>	<b><math>R^2</math></b>	<b><math>K_{\text{ads}}</math> (M<sup>-1</sup>)</b>	<b><math>\Delta G^{\circ}_{\text{ads}}</math> (kJ mol<sup>-1</sup>)</b>
Hydrogen evolution	0.9985	1428	-28.36
Electrochemical	0.9991	1666	-28.75

**Table 4:** The heat of adsorption ( $Q_{\text{ads}}$ ) of L-Serine on Pb surface in 5.0 M  $\text{H}_2\text{SO}_4$  at various concentrations of L-Serine

L-Serine (mM)	$\theta_1$	$\theta_2$	$Q_{\text{ads}}$ ( $\text{kJ mol}^{-1}$ )
	303 K	323 K	
0.1	0.080	0.052	-18.64
0.5	0.320	0.289	-6.51
1	0.720	0.631	-16.57
5	0.840	0.763	-19.93
10	0.880	0.789	-27.43
15	0.880	0.815	-20.67
20	0.880	0.815	-20.67

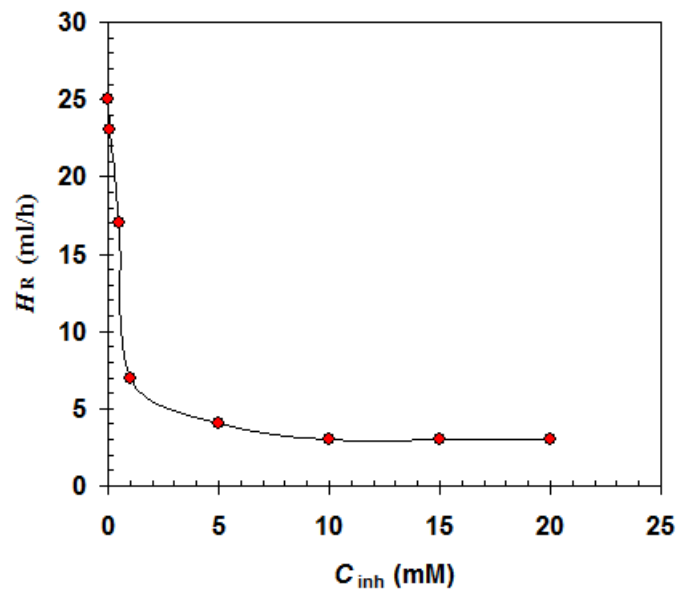


Fig. 1

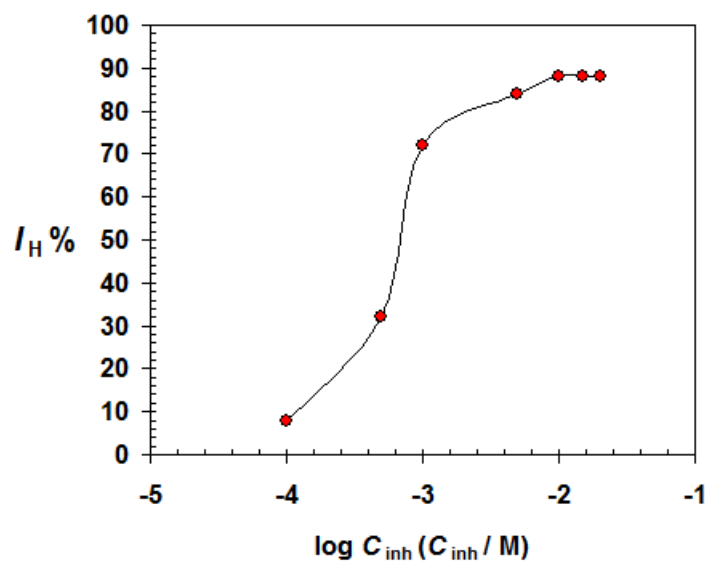


Fig.2

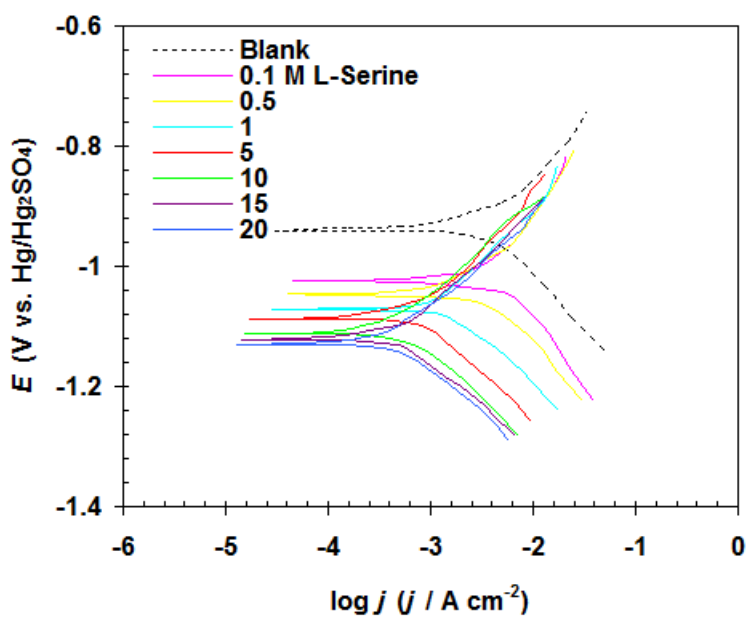


Fig. 3

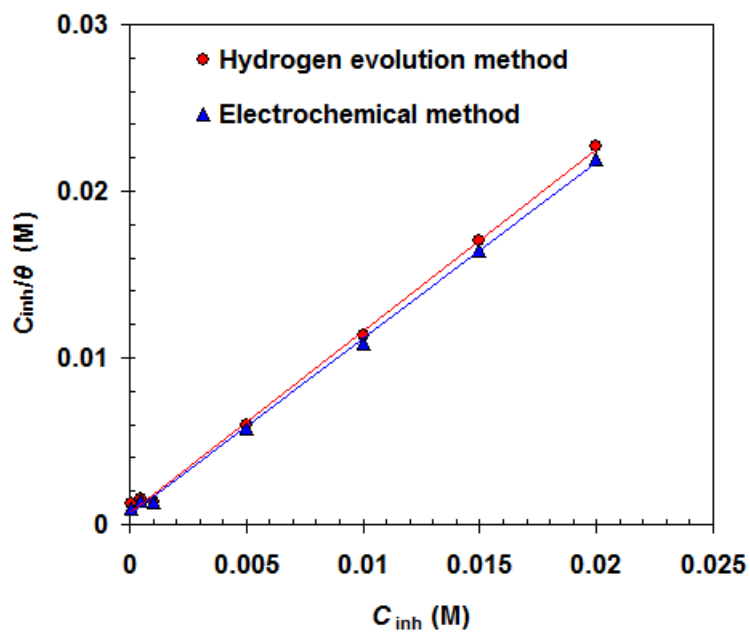


Fig .4

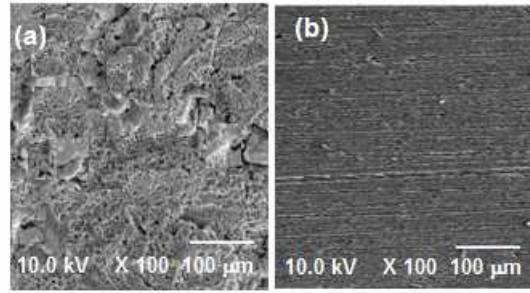


Fig.5

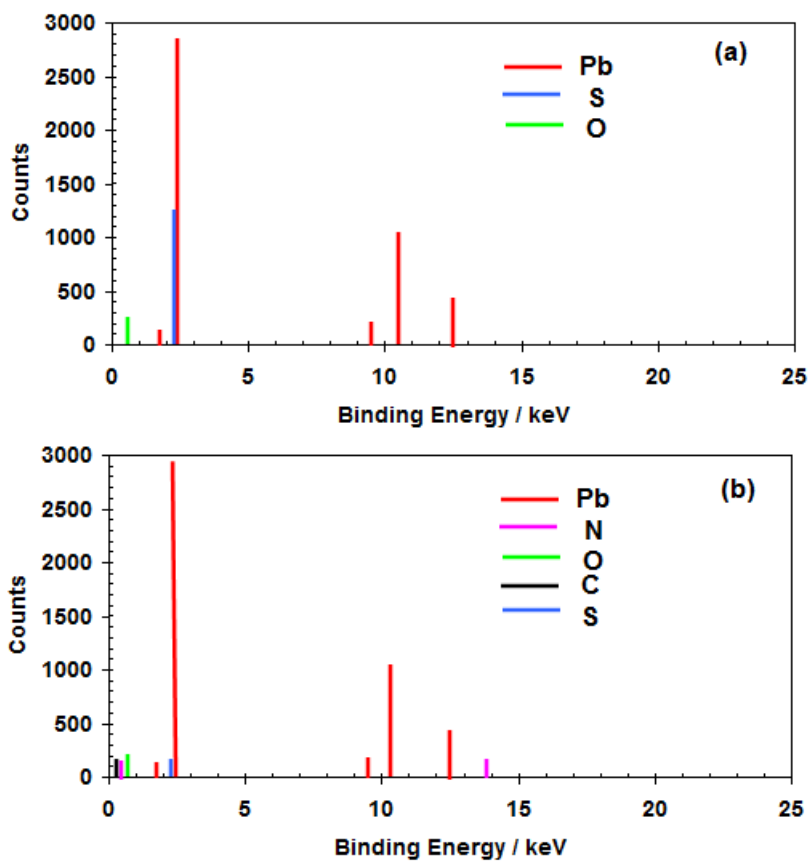


Fig.6

